

Apr 14th, 12:00 AM - 12:00 AM

## Multi-Modality Breast MRI Segmentation Using nn-UNet for Preoperative Planning of Robotic Surgery Navigation

Motaz Alqaoud  
*Old Dominion University*

John Plemmons MD  
*Eastern Virginia Medical School*

Eric Feliberti MD, FACS  
*Eastern Virginia Medical School*

Krishnanand Kaipa  
*Old Dominion University*

Siqin Dong  
*Old Dominion University*

*See next page for additional authors*

Follow this and additional works at: <https://digitalcommons.odu.edu/msvcapstone>



Part of the [Biomedical Engineering and Bioengineering Commons](#), [Robotics Commons](#), and the [Surgery Commons](#)

---

### Recommended Citation

Alqaoud, Motaz; Plemmons, John MD; Feliberti, Eric MD, FACS; Kaipa, Krishnanand; Dong, Siqin; Fichtinger, Gabor; Xiao, Yimming; and Audette, Michel, "Multi-Modality Breast MRI Segmentation Using nn-UNet for Preoperative Planning of Robotic Surgery Navigation" (2022). Modeling, Simulation and Visualization Student Capstone Conference. 2. DOI: 10.25776/zz2y-x338 <https://digitalcommons.odu.edu/msvcapstone/2022/medical/2>

This Paper is brought to you for free and open access by ODU Digital Commons. It has been accepted for inclusion in Modeling, Simulation and Visualization Student Capstone Conference by an authorized administrator of ODU Digital Commons. For more information, please contact [digitalcommons@odu.edu](mailto:digitalcommons@odu.edu).

---

**Author/s**

Motaz Alqaoud; John Plemmons MD; Eric Feliberti MD, FACS; Krishnanand Kaipa; Siqin Dong; Gabor Fichtinger; Yimming Xiao; and Michel Audette

# MULTI-MODALITY BREAST MRI SEGMENTATION USING NN-UNET FOR PREOPERATIVE PLANNING OF ROBOTIC SURGERY NAVIGATION

Motaz Alqaoud

Biomedical Engineering  
Old Dominion University  
5115 Hampton Blvd  
Norfolk, VA, USA  
[malqa004@odu.edu](mailto:malqa004@odu.edu)

Krishnanand Kaipa  
Siqin Dong

Mechanical & Aerospace Engineering  
Old Dominion University  
5115 Hampton Blvd  
Norfolk, VA, USA  
[kkaipa@odu.edu](mailto:kkaipa@odu.edu), [sdong002@odu.edu](mailto:sdong002@odu.edu)

Yiming Xiao

Computer Science & Software Engineering  
Concordia University  
1455 Boulevard de Maisonneuve O  
Montreal, QC, Canada  
[yiming.xiao@concordia.ca](mailto:yiming.xiao@concordia.ca)

John Plemmons  
Eric Feliberti

Dept. of Radiology & Dept. of Surgery  
Eastern Virginia Medical School  
825 Fairfax Ave  
Norfolk, VA, USA  
[jklepmon@gmail.com](mailto:jklepmon@gmail.com), [felibee@evms.edu](mailto:felibee@evms.edu)

Gabor Fichtinger

School of Computing  
Queen's University  
99 University Ave  
Kingston, ON, Canada  
[fichting@queensu.ca](mailto:fichting@queensu.ca)

Michel Audette

Computational Modeling & Simulation  
Engineering  
Old Dominion University  
5115 Hampton Blvd  
Norfolk, VA, USA  
[maudette@odu.edu](mailto:maudette@odu.edu)

## ABSTRACT

Segmentation of the chest region and breast tissues is essential for surgery planning and navigation. This paper proposes the foundation for preoperative segmentation based on two cascaded architectures of deep neural networks (DNN) based on the state-of-the-art nnU-Net. Additionally, this study introduces a polyvinyl alcohol cryogel (PVA-C) breast phantom based on the segmentation of the DNN automated approach, enabling the experiments of navigation system for robotic breast surgery. Multi-modality breast MRI datasets of T2W and STIR images were acquired from 10 patients. Segmentation evaluation utilized the Dice Similarity Coefficient (DSC), segmentation accuracy, sensitivity, and specificity. First, a single class labeling was used to segment the breast region. Then it was employed as an input for three-class labeling to segment fat, fibroglandular (FGT) tissues, and tumorous lesions. The first architecture has a 0.95 DCS, while the second has a 0.95, 0.83, and 0.41 for fat, FGT, and tumor classes, respectively.

**Keywords:** MRI segmentation, convolutional neural networks, breast surgery, surgery planning,

## 1 INTRODUCTION

Breast cancer is the most common cancer among women, except skin cancer (Torre et al. 2015). While the primary treatment is breast-conserving surgery (BCS), breast cancers can be spotted on a screening X-ray mammogram (XRM) as a nonpalpable abnormality, enabling less invasive local treatment. However, tumor localization is necessary to guide surgical excision (Frank, Hall, and Steer 1976); existing approaches have limited visualization in the procedure; a radiologist inserts a wire marker into the tumor prior to the surgical excision, which is determined by 2D guidance founded on a projection XRM (St John et al. 2017). Subsequently, the surgeon uses the guidewire to localize the tumor through XRM annotations by the radiologist and possibly aided by 2D ultrasound (US). Hence, the wire marker usually offers poor localization of the resection area, particularly for nonpalpable tumors, frequently leading to inaccurate localization and imprecise excision, which contributes to sizeable healthy tissue resections, tumor spillage, and spreading the resection border (Torre et al. 2015).

Additionally, navigation towards complex 3D lesions visualization is frequently accomplished with 2D freehand US (FUS) (Krücker et al. 2011). Yet, localization cannot be adequately visualized due to the poor image contrast of the US. Although highly sensitive imaging modalities (such as MRI) can be used in a preoperative procedure to obtain precise positions of the lesions, finding a method to update and align these lesions' positions from real-time US images can benefit current surgical procedures. Therefore, many research and commercial platforms have applied image fusion techniques that align preoperative and intraoperative images, utilizing rigid or affine registration techniques (Guo et al. 2018). Hence, the breast is hyperelastic anatomy; applying compression forces by the US probe would entail a considerable nonlinear deformation challenge. Therefore, an applicable alignment procedure of the preoperative and intraoperative US images is vital for an actual probe-tissue coupling and sufficient image quality. However, a proper soft tissue modeling of breast elasticity in real-time has not been solved.

This paper describes a deep learning (DL) approach of multi-modality breast MRI segmentation that can be used as the foundation for preoperative imaging in a future combination with intraoperative imaging in a surgery navigation system. Consequently, magnetic resonance imaging (MRI) of the breast is becoming very beneficial for diagnosing and screening breast cancer (Sinha and Sinha 2009). Due to its high soft-tissue contrast, MRI can detect the discrimination between different structures in the breast and enable 3D visualization (Giess et al. 2014). However, breast MRI imaging includes other organs such as the lung, heart, and pectoral muscles. As a result, it is crucial to segment the breast region from the other organs.

Moreover, segmentation is essential in many clinical applications (Aerts et al. 2014, Nestle et al. 2005), such as interventional treatments and intra-operative surgery navigation systems (Bernard et al. 2018). However, MRI manual segmentation is time-demanding and user variability-dependent (Granzier et al. 2020). Therefore, numerous techniques have been developed to help radiologists diagnose, detect, and enhance the analysis efficacy of the breast lesion (Pang et al. 2015). Semi-automated methods (Chen, Giger, and Bick 2006) need less time than manual methods, but they still require user involvement, yielding varying results depending on different users. Yet, fully automated segmentation of breast tissue and lesions continues to be a challenge even by using computer-aided diagnosis (CAD) systems (Gubern-Mérida et al. 2015).

Various traditional algorithms have been utilized to address this problem. For example, Fuzzy c-mean (FCM) is used for lesion detection, where voxels are assigned into classes based on their distance in the feature space has been used in lesion detection (Bezdek 1981, Chen, Giger, and Bick 2006) Wu et al. (Wu et al. 2013) developed an edge technique in the 3D sagittal T1-weighted MRI scans to segment the breast region out from other organs and achieved a DSC of 0.95. In recent years, deep learning techniques have been largely used in medical image segmentation tasks, for instance, Fully Convolutional Network FCN (Shelhamer, Long, and Darrell 2017), SegNet (Badrinarayanan, Kendall, and Cipolla 2017), U-Net (Ronneberger, Fischer, and Brox 2015), and V-Net (Milletari, Navab, and Ahmadi 2016). These DNNs can extract detailed features and accomplish end-to-end segmentation. (Zhang et al. 2019) developed a DL

approach using U-Net for breast region and FGT segmentation, achieving a DSC of 0.86 and 0.83, respectively.

However, most traditional and DL segmentation models require modification for specific datasets. Thus, the DNN parameters are often fine-tuned for particular MRI scanner characteristics and protocols. Therefore, different modalities and scanning protocols yield different breast MRI scans. Although existing approaches have shown an acceptable performance on specific task optimization problems, they may not handle the variability of MRI data.

Therefore, we propose applying two consecutive nnU-Net architectures for the breast region, inner breast tissues, and tumor masses segmentation by using multi-modality breast tumor images. This will cope with the variability of MRI data and avoid manual intervention. nnU-Net has appeared as a state-of-the-art biomedical segmentation architecture (Isensee et al. 2021). It is a self-adapted network architecture method for every particular image dataset. Without manual tuning or user intervention, nnU-Net configure all the segmentation task stages, resulting in performance optimization for every dataset. This architecture exhibited an outstanding performance for the task-specialized DL pipelines of 33 international public segmentation competitions (Isensee et al. 2021). Likewise, it has been widely applied to many segmentation competitions, but it has not been applied to multi-modality breast cancer MRI datasets yet. To the best of our knowledge, this study is the first to explore and test nnU-Net for breast region and 3-class breast tissue segmentation for fat, FGT, and tumor mass in a routine MRI dataset that consists of 10 T2-weighted and STIR fat-suppressed multi-modality images gained from an open-access breast MRI database.

Furthermore, we are also presenting a patient-specific breast-mimicking phantom based on that automated segmentation approach. It will allow the experiments of developing and validating a calibration-assisted preoperative MRI to intraoperative 3D US registration technique utilizing an open-source PLUS toolkit (Lasso et al. 2014). This registration will integrate later with the optical tracking of a breast surgery robot. Validation will use surgical fiducials markers inserted in a breast phantom.

## **2 MATERIALS AND METHODS**

### **2.1 Datasets**

The datasets of this study contain 10 patients (median age, 40 years; range, 40-70 years). All subjects are acquired from an open-source cancer imaging archive ([www.cancerimagingarchive.net](http://www.cancerimagingarchive.net)) under the breast-diagnosis study category. We select each subject dataset consisting of two MR modalities: T2-weighted and STIR fat-suppressed images. Each breast image volume consists of 82 to 95 axial slices with a slice thickness of 2 mm. variant of pixel resolution, and image sizes are noted on the selected dataset. As a result, we resample to the pixel resolution of 0.65 mm along x and y, and image size of  $512 \times 512$ . Patients are scanned in the prone position while their breasts are hanging in the two holes of the 1.5 T Philips MRI scanner coil. Thus, we randomly split the dataset to 80:20, where 8 image volumes were assigned for training/validation and 2 image volumes for testing. Therefore, a trained biomedical engineer has manually produced the ground truth (GT) segmentation to generate a reference for breast region, fat, FGT, and tumor since there is insufficient data analysis in online repositories. This manual segmentation is revised and validated by a radiologist from Eastern Virginia Medical School (EVMS) in Norfolk, VA. The manual segmentation on 3D Slicer 4.11(Fedorov et al. 2012) platform is used for this purpose.

### **2.2 Segmentation based on nnU-Net**

We build our pipeline network based on nnU-Net—the two cascaded nnU-Net architectures with multimodal inputs of T2-weighted and STIR fat-suppressed MRI modalities. Our cascaded nnU-Net approach is first to binarize the whole breast region and then use these masks as input for the second network to perform three-class segmentation of fat tissue, FGT tissue, and tumor mass within the breast region. Figure 1 illustrates the proposed segmentation framework where the upper rectangle illustrates the breast region segmentation, and the lower rectangle depicts the inner breast tissues segmentation.

The nnU-Net architecture is adapted from 3D U-Net (Ronneberger, Fischer, and Brox 2015, Isensee et al. 2021, Çiçek et al. 2016). It consists of a contracting network cascaded with an expansive network, which confers a U-shaped structure.

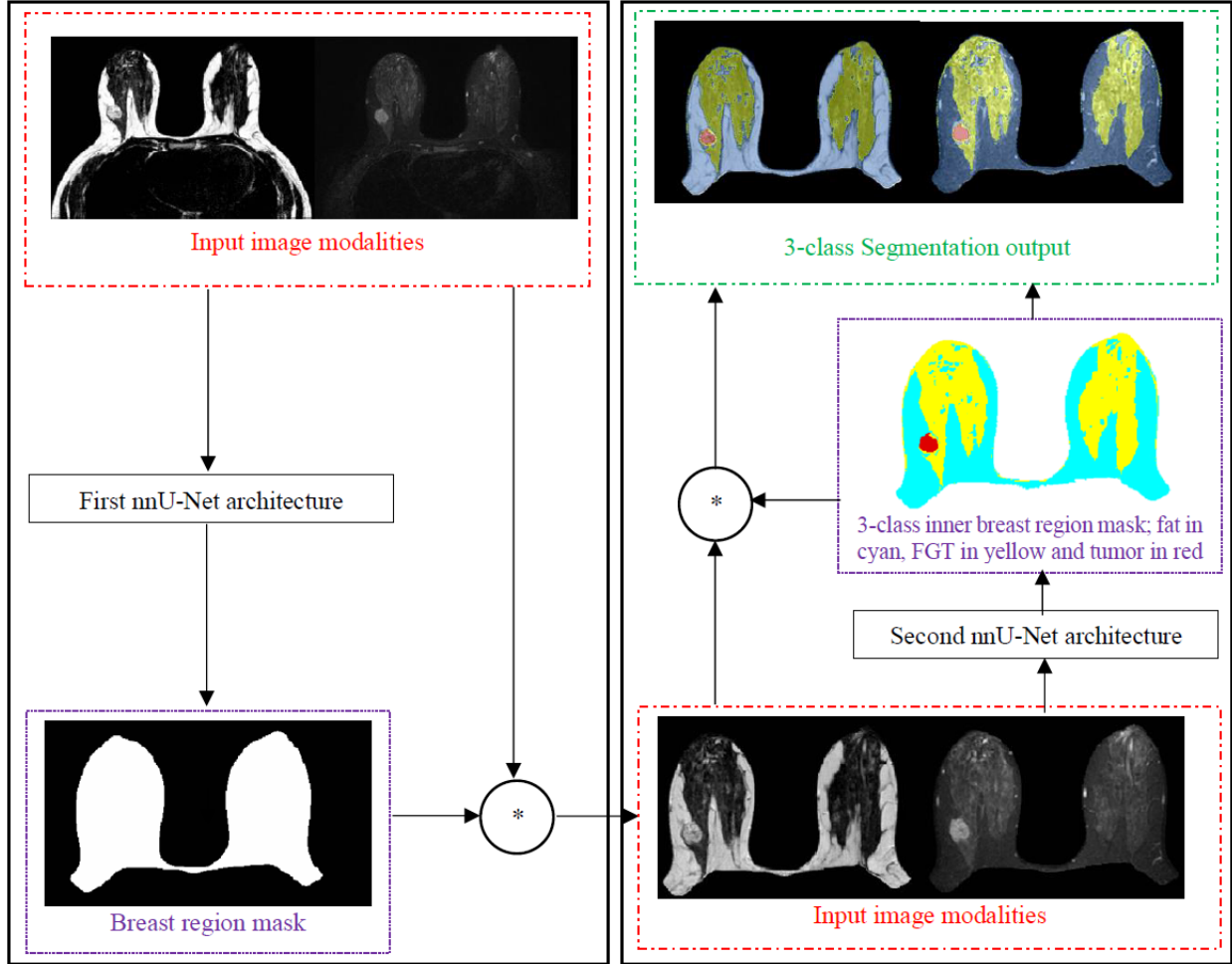


Figure 1. The pipeline of two cascaded nnU-Net architectures where the left rectangle is the breast region segmentation, and the right rectangle is the inner breast tissues segmentation.

It consists of a contracting network cascaded with an expansive network, which confers a U-shaped structure. The contracting pathway, coinciding with the downslope of the U, embeds the repeated application of a convolution, a Leaky Rectified Linear Unit (Leaky ReLU), and a max-pooling operation, where the spatial information is decreased, and feature-based representation is increased. The expansive pathway, which marks the upslope, combines features and spatial data by deconvolutions series for high-resolution features from the contracting path over successive layers (Ronneberger, Fischer, and Brox 2015). As a result, the skip connection between the corresponding contracting and expansive paths layers retains the accurate feature information vital for the up-sampled output image. Therefore, at the final layer of the expansive pathway, a convolution with a  $1 \times 1 \times 1$  kernel is performed up-sampling so that the segmentation voxel results correspond to the voxel input image (Isensee et al. 2021). Figure 2 illustrates the network parameters and their datasets. Rather than a regular cross-entropy loss function, nnU-Net uses a combination of cross-entropy loss and dice loss functions to train one class label and three class labels for the first and second network, respectively. Because of that, the segmentation accuracy and training stability are improved (Isensee et al. 2021). In addition, eight operations of data augmentation are implemented by nnU-Net to cope with our limited training data, such as scaling, rotation, Gaussian noise, and Gaussian blur and mirroring (Isensee et al. 2021). It is worth mentioning that nnU-Net embeds some refinements to the

U-Net architecture baseline (Ronneberger, Fischer, and Brox 2015, Isensee et al. 2021), namely: (1) convolution padding to maintain the exact image size for inputs and outputs; (2) use of instance normalization (IN) as a substitute for batch normalization; (3) instead of ReLU, Leaky ReLU is used to address the dying neuron issue. Also, nnU-Net is a self-configurable algorithm where cropping, resampling, and normalization were executed to the dataset parameters such as slice thickness and resolution as a part of the nnU-Net preprocessing step (Isensee et al. 2021).

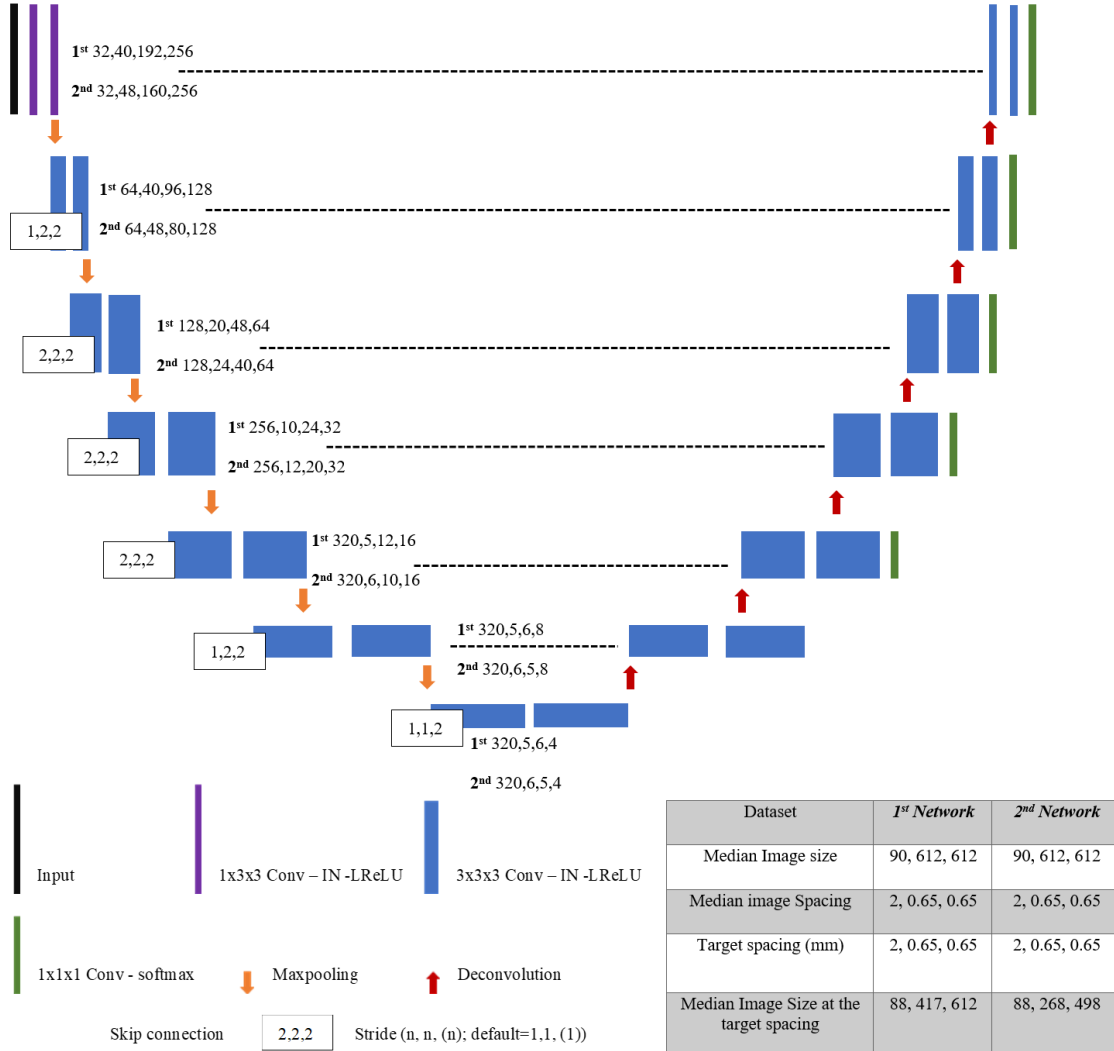


Figure 2. The nnU-Net architecture.

The nnU-Net model utilizes the stochastic gradient descent method with initial learning (0.01) and Nesterov Momentum (0.9) to optimize the loss function (Isensee et al. 2021). The patch sizes of the two nnU-Net networks are  $40 \times 192 \times 256$  and  $48 \times 160 \times 256$ , respectively, for the breast region and breast tissue segmentations. In this study, the minimum batch size is at 2, the minimum feature map size is at  $4 \times 4 \times 4$ , while the maximum number of feature map is at 320. Therefore, the down-sampling number is 6. All training runs are set for 1000 epochs, and each epoch consists of 250 batches. We apply 5-fold cross-validation (CV) for training and validation to exploit the manual GT segmentations we analyze and obtain from the breast MRI dataset's public repositories. The segmentation model is trained on ODU's High-Performance Computing cluster. A virtual environment based on python 3.8.5 was created in the cluster using PyTorch 1.6.0 (Paszke et al. 2019) as a framework. In addition, Batchgenerators 0.21 (Isensee 2020) and all other necessary python libraries were installed on the virtual environment. The nnU-Net code is publicly accessible at [github.com/MIC-DK-FZ/nnUNet](https://github.com/MIC-DK-FZ/nnUNet).

### 2.3 Evaluation

The performance of the segmentation network of cascaded architecture is evaluated with standard statistical metrics of segmentation, DSC, and assessments of accuracy, sensitivity, and specificity (Tharwat 2021, Popovic et al. 2007).

$$DSC = \frac{2 \times TP}{2 \times TP + FP + TP + FN} \quad (1)$$

$$Accuracy = \frac{TP + TN}{TP + FP + TN + FN} \quad (2)$$

$$Sensitivity = \frac{TP}{TP + FN} \quad (3)$$

$$Specificity = \frac{TN}{TN + FP} \quad (4)$$

Where, TP, TN, FP, and FN represent true positive, true negative, false positive, and false negative, respectively.

### 2.4 Segmentation-guided elastic breast phantom application

we build a breast phantom based on the DL automated breast segmentation approach for our robotic surgery application navigation experiments. We have created Polyvinyl Alcohol Cryogel (PVA-C) breast phantoms started on our segmentation results. We opt for PVA-C because it shows elastic fidelity, mimicking soft tissue deformations and medical imaging properties (Surry et al. 2004). PVA-C is a blended mixture of PVA powder in deionized water that is first heated to stimulate a complete dissolution. Then it becomes an elastic solid by frozen and thawed cycles one or more times. Additionally, we can control imaging and elastic properties by controlling the PVA concentrations and the number of freeze-thaw cycles (FTC) (Surry et al. 2004). It is worth noting that 3D printing is a crucial component of the PVA-C molds; the planning and navigation experiments need a highly compatible soft tissue phantom, which disqualifies most 3D-printed options in our case.

Polyvinyl alcohol (PVA) powder with an average molecular weight (MW) of 130,000 and the hydrolysis of over 99% (Sigma-Aldrich, SKU 563900) is used for the preparation of aqueous liquids. Our method and approach are centered on the published methods of (Surry et al. 2004) and (Kharine et al. 2003). Therefore, a 90 wt. % deionized water and 10 wt.% PVA powder is combined in an Erlenmeyer flask. Hence, we write down the flask weight and its contents. Then, we use a magnetic stir plate to blend the mixture for 30 minutes. Then, the solution is taken to a 95°C temperature bath for 2 h. to break down any masses. After that, we lightly stir PVA for 1 hour to promote dissolution and solution homogeneity and gradually cooled down to room temperature. Lastly, the flask is weighed one last time to restore any weight loss by deionized water, so the solution weight remains to have a 10 wt—% PVA.

In order to make an anthropomorphic elastic phantom, the PVA liquid must be poured into the proper molds. Hence, these molds are 3D-printed from surfaces extracted of our segmentation results. Therefore, we create molds for tissue-mimicking fat, FGT, and tumors. Accordingly, we use open-source 3D Slicer 4.11 (Fedorov et al. 2012) to extract surfaces from segmented tissue.

30 ml of liquid PVA are colored with red enamel paint (Testor's 1105tt, red metallic paint) and 320 ml with yellow paint (Testor's 1115TT, amber metallic paint). Thus, colored PVA-C visually indicates the tumor and FGT-mimicking tissue boundaries, respectively. We then dispense the red-colored liquid PVA into its mold and let it rest for 12 hours, allowing air bubbles to rise and dissipate. We keep it well-sealed at room temperature during this time. Soon later, the freezing phase begins in a standard chest freezer, starting from room temperature till gradually reaching  $-20^{\circ}\text{C}$  over 12 h. Accordingly, the thawing phase is initiated by turning off the freezer, and gradually the temperature goes to room temperature over 12 hours. In this manner, one FTC is finished. Then, a second FTC is initiated for the tumor-mimicking volume. The yellow-colored liquid PVA is poured into its mold for its first FTC.

Later, the tumor and FGT components are separated from their molds and placed inside the fat-mimicking mold to complete the making of the breast phantom. Therefore, we sew a nylon thread over the tumor and

FGT mimicking volumes so that they are hanging in the fat mimicking volume mold to make certain of the distance and spatial coherence of the three components. Next, the fat-mimicking volume container is loaded with PVA liquid. Finally, we place it in the freezer for a last FTC. Once it is finished, we cut out the threads. Thus, the phantom is separated from its mold as we have a breast-mimicking phantom that contains 1 FTC for Fat-mimicking tissue, 2 FTCs for the FGT component, and 3 FTCs for the tumor. Therefore, we can store it in deionized water at 5 °C (Surry et al. 2004).

### 3 RESULTS

We evaluated our pipeline method on the segmentation evaluation metrics described in section D. All results were shown in Table 1 as mean  $\pm$  SD. The reported results are from the highest model performance out of 5-fold CV. The DSC values for breast region, fat, FGT, and tumor segmentation are  $0.95 \pm 0.07$ ,  $0.95 \pm 0.00$ ,  $0.83 \pm 0.04$ , and  $0.41 \pm 0.58$  respectively.

Table 1. Performance Evaluation of The Two Networks\*.

Network/ Seg. task		DSG	Accuracy	Sensitivity	Specificity
1 <sup>st</sup> nnUNet	Breast region (Test dataset)	$0.95 \pm 0.00$ ( $0.95 \pm 0.00$ )	$0.98 \pm 0.00$ ( $0.99 \pm 0.00$ )	$0.95 \pm 0.03$ ( $0.96 \pm 0.02$ )	$0.99 \pm 0.00$ ( $0.99 \pm 0.00$ )
	Fat (Test dataset)	$0.95 \pm 0.00$ ( $0.96 \pm 0.00$ )	$0.99 \pm 0.00$ ( $0.99 \pm 0.00$ )	$0.98 \pm 0.02$ ( $0.96 \pm 0.04$ )	$0.99 \pm 0.00$ ( $0.99 \pm 0.00$ )
2 <sup>nd</sup> nnUNet	FGT (Test dataset)	$0.83 \pm 0.04$ ( $0.84 \pm 0.03$ )	$0.99 \pm 0.00$ ( $0.99 \pm 0.00$ )	$0.77 \pm 0.01$ ( $0.86 \pm 0.18$ )	$0.99 \pm 0.00$ ( $0.99 \pm 0.00$ )
	Tumor (Test dataset)	$0.41 \pm 0.58$ ( $0.35 \pm 0.48$ )	$0.99 \pm 0.00$ ( $0.99 \pm 0.00$ )	$0.45 \pm 0.64$ ( $0.33 \pm 0.45$ )	$0.99 \pm 0.00$ ( $0.99 \pm 0.00$ )

\*Results shown were from the fold 2 model among 5-fold CV.

Figure 3 showed a case of an image prediction of our DL method compared to the ground truth, as well as an applicable phantom is shown in Figure 4, which is made based on the segmentation results.

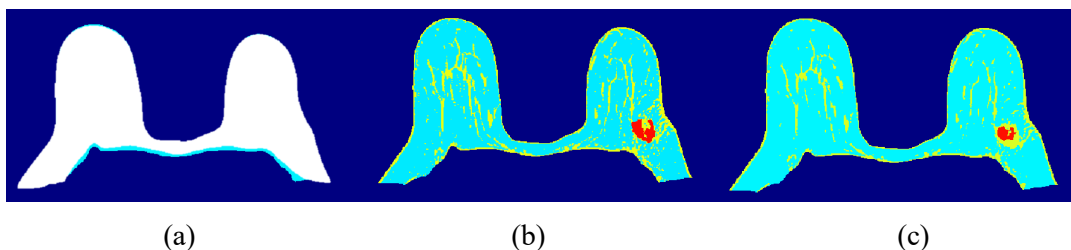


Figure 3. (a) the prediction case from the test dataset of the breast region mask in white overlaid on its ground truth. (b) GT of the 3-class segmentation shows fat tissue in light blue, FGT in yellow, and tumor in red. (c) shows the prediction from the test dataset of the 3-class segmentation of the same case of (b).

Our breast segmentation task is implemented through two cascaded networks. We employed 5-fold CV models for every network. One model of breast region and 3-class inner tissue segmentation networks took on average of 145 s and 170 s respectively for one epoch during model training. In addition, every model took less than two days (40 h and 47 h) for the complete training process.

### 4 DISCUSSION AND FUTURE WORK

We exhibited a DL approach to address the clinical need to segment breast tissues and establish a foundation for image navigation since traditional methods do not provide good performance to separate the breast

region and label breast tissues. Thus, our segmentation pipeline has two consecutive networks of nnU-Net architecture. Accordingly, we used the trained model and the segmentation results to develop a PVAC breast phantom to support and experiment with navigation surgery studies.

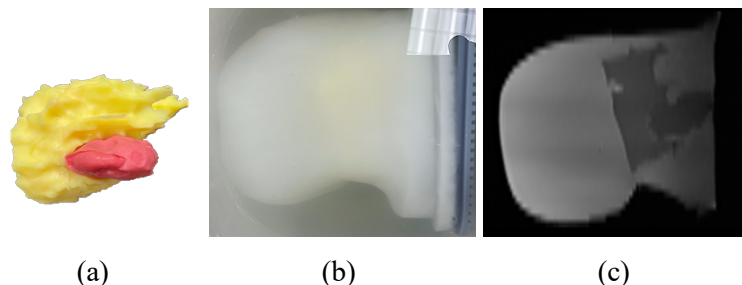


Figure 4. indicates the developed PVA-C breast phantom based on segmentation results, where, at (a). the yellow represents the segmented volume of FGT, and the red represents the tumor volume. (b) one breast of PVA-C breast phantom mimics fat, FGT, and tumor. (c) PVA-C breast phantom MRI.

We used an open-source for our dataset that included MRI images of T2W/STIR of 10 patients. As shown in Table 1, our pipeline confirmed high accuracy, high sensitivity, and specificity, preventing over-segmentation and preserving segmentation sensitivity.

We evaluated our findings to other deep-learning methods, as shown in Table 2. (Dalmış et al. 2017, Jiao et al. 2020). Therefore, our pipeline had accomplished exceptional performance with a smaller dataset, specifically for breast region and fat segmentation with a DSC value of 0.95 and 0.95, respectively. However, the DSC values of literature (Dalmış et al. 2017, Jiao et al. 2020) in Table 2 were near to our results, but the training cases were much more than ours, and their segmentation object is for two regions.

Table 2. DSC Values Comparison of Our Method and Other Literature\*.

Author	Method, number of the training dataset		Segmentation tasks			
			Breast Region	Fat	FGT	Tumor sensitivity
Damlis et al. (Dalmış et al. 2017)	2-D U-Net	66	$0.94 \pm 0.00$	-	$0.81 \pm 0.01$	-
Jiao et al. (Jiao et al. 2020)	U-Net ++	75	$0.95 \pm 0.00$	-	-	0.87
Ours	3-D nnU-Net	8	$0.95 \pm 0.00$	$0.95 \pm 0.00$	$0.83 \pm 0.04$	0.45

\* For comparison purposes, tumor sensitivity results were shown.

The tumor segmentation showed DSC and sensitivity of 0.41 and 0.45, respectively, implying that a considerable tumor mass was wrongly unsegmented (i.e., high false negative). Yet, expanding the training dataset is expected to support overcoming this challenge and improve the segmentation performance even more.

This work presents the foundation of preoperative images to develop a breast surgery navigation system by intruding DL segmentation pipeline built on the nnU-Net for breast region, fat, FGT, and tumor segmentation. Our group is working on a real-time tracking system for breast tumors using DCNN for pre- and intra-operative imaging. Our pipeline plan will allow us to update in real-time the boundary position of breast tumors based on a patient-specific model by relating preoperative scans on US images, enabling constant visualization. As we showed in this study the stage of the preoperative image, our intraoperative stage consists of MRI-US image registration, which also leverages a nnU-Net architecture, this time for synthesizing finite elements. Moreover, the intraoperative stage will employ a combination of MRI-US image registration, optical tracking, and surgical robotic integration. It will be completed in three steps. 1)

MRI-US calibration 2) MRI-US fiducials-based point-cloud affine registration 3) DL-based elastic registration Figure 5. Our navigation system will create a real-time soft-tissue tracking system to improve tumor localization during surgical procedures. The position of lesions localized on preoperative images segmentation will be updated from intraoperative ultrasound data and visualized by the surgeon in real-time. Our robotic surgery design is proposed by co-author (K.K); it is a hand-held grasping robot equipped with multiple claws that are embedded in a balloon-like covering to perform tumor resection with spillage-free.

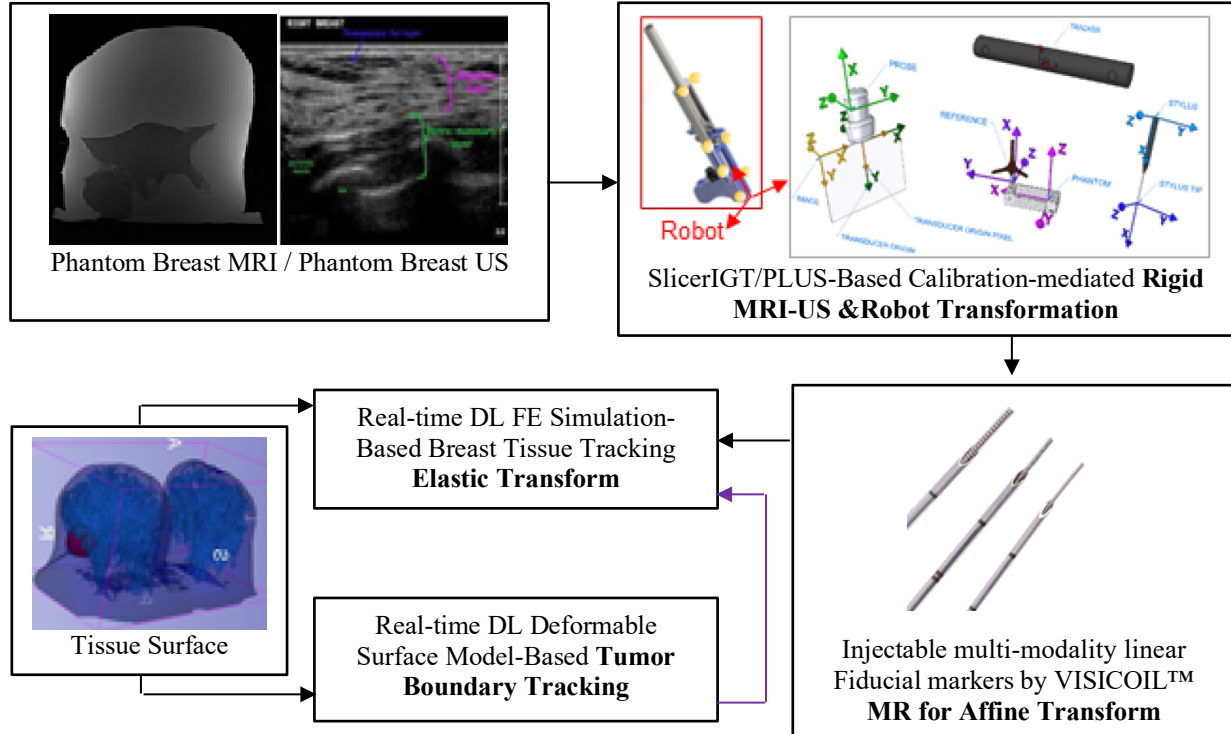


Figure 5. intraoperative DL-based MRI-US registration stage.

Our study has some limitations. Our small dataset of 10 patients will expand in future work to improve the performance and reliability. Another limitation is that we used MRI scans from an online repository with no control over MRI scanning protocols. However, even with these limitations, our framework enabled us to present impressive results and show the potential capabilities of cascaded nnU-Net architectures.

## 5 CONCLUSION

This paper described the preoperative DL segmentation pipeline stage for preoperative breast surgery planning from MRI, built on the nnU-Net. In addition, we introduced a mimicking breast phantom created on these segmentation results. We used multi-modality breast MRI datasets obtained from a public archive. The nnUNet-based pipeline showed high segmentation accuracy across routine breast MR images without fine-tuning or post-processing steps. In short, this study establishes the base for developing and validating robotic experiments of the intra-operative navigation system based on 3DUS. Elastic MRI-3DUS registration, as well as based on DNNs, for finite elements synthesis, which will be emphasized in the near future.

## ACKNOWLEDGMENTS

This work was supported by Old Dominion University (Biomedical Engineering) and by Eastern Virginia Medical School.

## REFERENCES

- Aerts, H. J., E. R. Velazquez, R. T. Leijenaar, C. Parmar, P. Grossmann, S. Carvalho, J. Bussink, R. Monshouwer, B. Haibe-Kains, D. Rietveld, F. Hoebers, M. M. Rietbergen, C. R. Leemans, A. Dekker, J. Quackenbush, R. J. Gillies, and P. Lambin. 2014. "Decoding tumour phenotype by noninvasive imaging using a quantitative radiomics approach." *Nat Commun* 5:4006. doi: 10.1038/ncomms5006.
- Badrinarayanan, V., A. Kendall, and R. Cipolla. 2017. "SegNet: A Deep Convolutional Encoder-Decoder Architecture for Image Segmentation." *IEEE Transactions on Pattern Analysis and Machine Intelligence* 39 (12):2481-2495. doi: 10.1109/TPAMI.2016.2644615.
- Bernard, O., A. Lalande, C. Zotti, F. Cervenansky, X. Yang, P. A. Heng, I. Cetin, K. Lekadir, O. Camara, M. A. Gonzalez Ballester, G. Sanroma, S. Napel, S. Petersen, G. Tziritas, E. Grinias, M. Khened, V. A. Kollerathu, G. Krishnamurthi, M. M. Rohé, X. Pennec, M. Sermesant, F. Isensee, P. Jäger, K. H. Maier-Hein, P. M. Full, I. Wolf, S. Engelhardt, C. F. Baumgartner, L. M. Koch, J. M. Wolterink, I. Išgum, Y. Jang, Y. Hong, J. Patravali, S. Jain, O. Humbert, and P. M. Jodoin. 2018. "Deep Learning Techniques for Automatic MRI Cardiac Multi-Structures Segmentation and Diagnosis: Is the Problem Solved?" *IEEE Transactions on Medical Imaging* 37 (11):2514-2525. doi: 10.1109/TMI.2018.2837502.
- Bezdek, James. 1981. *Pattern Recognition With Fuzzy Objective Function Algorithms*.
- Chen, W., M. L. Giger, and U. Bick. 2006. "A fuzzy c-means (FCM)-based approach for computerized segmentation of breast lesions in dynamic contrast-enhanced MR images." *Acad Radiol* 13 (1):63-72. doi: 10.1016/j.acra.2005.08.035.
- Çiçek, Özgün, Ahmed Abdulkadir, Soeren S. Lienkamp, Thomas Brox, and Olaf Ronneberger. 2016. "3D U-Net: Learning Dense Volumetric Segmentation from Sparse Annotation." *Medical Image Computing and Computer-Assisted Intervention – MICCAI 2016, Cham, 2016//*.
- Dalmış, M. U., G. Litjens, K. Holland, A. Setio, R. Mann, N. Karssemeijer, and A. Gubern-Mérida. 2017. "Using deep learning to segment breast and fibroglandular tissue in MRI volumes." *Med Phys* 44 (2):533-546. doi: 10.1002/mp.12079.
- Fedorov, A., R. Beichel, J. Kalpathy-Cramer, J. Finet, J. C. Fillion-Robin, S. Pujol, C. Bauer, D. Jennings, F. Fennessy, M. Sonka, J. Buatti, S. Aylward, J. V. Miller, S. Pieper, and R. Kikinis. 2012. "3D Slicer as an image computing platform for the Quantitative Imaging Network." *Magn Reson Imaging* 30 (9):1323-41. doi: 10.1016/j.mri.2012.05.001.
- Frank, H. A., F. M. Hall, and M. L. Steer. 1976. "Preoperative localization of nonpalpable breast lesions demonstrated by mammography." *N Engl J Med* 295 (5):259-60. doi: 10.1056/nejm197607292950506.
- Giess, Catherine S., Eren D. Yeh, Sughra Raza, and Robyn L. Birdwell. 2014. "Background Parenchymal Enhancement at Breast MR Imaging: Normal Patterns, Diagnostic Challenges, and Potential for False-Positive and False-Negative Interpretation." *RadioGraphics* 34 (1):234-247. doi: 10.1148/rg.341135034.
- Granzier, R. W. Y., N. M. H. Verbakel, A. Ibrahim, J. E. van Timmeren, T. J. A. van Nijnatten, R. T. H. Leijenaar, M. B. I. Lobbes, M. L. Smidt, and H. C. Woodruff. 2020. "MRI-based radiomics in breast cancer: feature robustness with respect to inter-observer segmentation variability." *Sci Rep* 10 (1):14163. doi: 10.1038/s41598-020-70940-z.
- Gubern-Mérida, A., R. Martí, J. Melendez, J. L. Hauth, R. M. Mann, N. Karssemeijer, and B. Platel. 2015. "Automated localization of breast cancer in DCE-MRI." *Med Image Anal* 20 (1):265-74. doi: 10.1016/j.media.2014.12.001.
- Guo, R., G. Lu, B. Qin, and B. Fei. 2018. "Ultrasound Imaging Technologies for Breast Cancer Detection and Management: A Review." *Ultrasound Med Biol* 44 (1):37-70. doi: 10.1016/j.ultrasmedbio.2017.09.012.
- Isensee, Fabian and Jäger, Paul and Wasserthal, Jakob and Zimmerer, David and Petersen, Jens and Kohl, Simon and Schock, Justus and Klein, Andre and Roß, Tobias and Wirkert, Sebastian and Neher,

- Peter and Dinkelacker, Stefan and Köhler, Gregor and Maier-Hein, Klaus H. 2020. batchgenerators - a python framework for data augmentation. Zenodo.
- Isensee, Fabian, Paul F. Jaeger, Simon A. A. Kohl, Jens Petersen, and Klaus H. Maier-Hein. 2021. "nnU-Net: a self-configuring method for deep learning-based biomedical image segmentation." *Nature Methods* 18 (2):203-211. doi: [10.1038/s41592-020-01008-z](https://doi.org/10.1038/s41592-020-01008-z).
- Jiao, Han, Xinhua Jiang, Zhiyong Pang, Xiaofeng Lin, Yihua Huang, and Li Li. 2020. "Deep Convolutional Neural Networks-Based Automatic Breast Segmentation and Mass Detection in DCE-MRI." *Computational and Mathematical Methods in Medicine* 2020:2413706. doi: [10.1155/2020/2413706](https://doi.org/10.1155/2020/2413706).
- Kharine, A., S. Manohar, R. Seeton, R. G. Kolkman, R. A. Bolt, W. Steenbergen, and F. F. de Mul. 2003. "Poly(vinyl alcohol) gels for use as tissue phantoms in photoacoustic mammography." *Phys Med Biol* 48 (3):357-70. doi: [10.1088/0031-9155/48/3/306](https://doi.org/10.1088/0031-9155/48/3/306).
- Krücker, J., S. Xu, A. Venkatesan, J. K. Locklin, H. Amalou, N. Glossop, and B. J. Wood. 2011. "Clinical utility of real-time fusion guidance for biopsy and ablation." *J Vasc Interv Radiol* 22 (4):515-24. doi: [10.1016/j.jvir.2010.10.033](https://doi.org/10.1016/j.jvir.2010.10.033).
- Lasso, A., T. Heffter, A. Rankin, C. Pinter, T. Ungi, and G. Fichtinger. 2014. "PLUS: open-source toolkit for ultrasound-guided intervention systems." *IEEE Trans Biomed Eng* 61 (10):2527-37. doi: [10.1109/tbme.2014.2322864](https://doi.org/10.1109/tbme.2014.2322864).
- Milletari, F., N. Navab, and S. Ahmadi. 2016. "V-Net: Fully Convolutional Neural Networks for Volumetric Medical Image Segmentation." 2016 Fourth International Conference on 3D Vision (3DV), 25-28 Oct. 2016.
- Nestle, U., S. Kremp, A. Schaefer-Schuler, C. Sebastian-Welsch, D. Hellwig, C. Rube, and C. M. Kirsch. 2005. "Comparison of different methods for delineation of 18F-FDG PET-positive tissue for target volume definition in radiotherapy of patients with non-Small cell lung cancer." *J Nucl Med* 46 (8):1342-8.
- Pang, Z., D. Zhu, D. Chen, L. Li, and Y. Shao. 2015. "A computer-aided diagnosis system for dynamic contrast-enhanced MR images based on level set segmentation and ReliefF feature selection." *Comput Math Methods Med* 2015:450531. doi: [10.1155/2015/450531](https://doi.org/10.1155/2015/450531).
- Paszke, Adam, Sam Gross, Francisco Massa, Adam Lerer, James Bradbury, Gregory Chanan, Trevor Killeen, Zeming Lin, Natalia Gimelshein, Luca Antiga, Alban Desmaison, Andreas Köpf, Edward Yang, Zach DeVito, Martin Raison, Alykhan Tejani, Sasank Chilamkurthy, Benoit Steiner, Lu Fang, Junjie Bai, and Soumith Chintala. 2019. "PyTorch: An Imperative Style, High-Performance Deep Learning Library." NeurIPS.
- Popovic, Aleksandra, Matias de la Fuente, Martin Engelhardt, and Klaus Radermacher. 2007. "Statistical validation metric for accuracy assessment in medical image segmentation." *International Journal of Computer Assisted Radiology and Surgery* 2 (3):169-181. doi: [10.1007/s11548-007-0125-1](https://doi.org/10.1007/s11548-007-0125-1).
- Ronneberger, Olaf, Philipp Fischer, and Thomas Brox. 2015. "U-Net: Convolutional Networks for Biomedical Image Segmentation." Medical Image Computing and Computer-Assisted Intervention – MICCAI 2015, Cham, 2015//.
- Shelhamer, E., J. Long, and T. Darrell. 2017. "Fully Convolutional Networks for Semantic Segmentation." *IEEE Trans Pattern Anal Mach Intell* 39 (4):640-651. doi: [10.1109/tpami.2016.2572683](https://doi.org/10.1109/tpami.2016.2572683).
- Sinha, S., and U. Sinha. 2009. "Recent advances in breast MRI and MRS." *NMR Biomed* 22 (1):3-16. doi: [10.1002/nbm.1270](https://doi.org/10.1002/nbm.1270).
- St John, E. R., R. Al-Khudairi, H. Ashrafian, T. Athanasiou, Z. Takats, D. J. Hadjiminias, A. Darzi, and D. R. Leff. 2017. "Diagnostic Accuracy of Intraoperative Techniques for Margin Assessment in Breast Cancer Surgery: A Meta-analysis." *Ann Surg* 265 (2):300-310. doi: [10.1097/sla.0000000000001897](https://doi.org/10.1097/sla.0000000000001897).
- Surry, K. J., H. J. Austin, A. Fenster, and T. M. Peters. 2004. "Poly(vinyl alcohol) cryogel phantoms for use in ultrasound and MR imaging." *Phys Med Biol* 49 (24):5529-46. doi: [10.1088/0031-9155/49/24/009](https://doi.org/10.1088/0031-9155/49/24/009).
- Tharwat, Alaa. 2021. "Classification assessment methods." *Applied Computing and Informatics* 17 (1):168-192. doi: [10.1016/j.aci.2018.08.003](https://doi.org/10.1016/j.aci.2018.08.003).

- Torre, L. A., F. Bray, R. L. Siegel, J. Ferlay, J. Lortet-Tieulent, and A. Jemal. 2015. "Global cancer statistics, 2012." *CA Cancer J Clin* 65 (2):87-108. doi: 10.3322/caac.21262.
- Wu, S., S. P. Weinstein, E. F. Conant, M. D. Schnall, and D. Kontos. 2013. "Automated chest wall line detection for whole-breast segmentation in sagittal breast MR images." *Med Phys* 40 (4):042301. doi: 10.1118/1.4793255.
- Zhang, Y., J. H. Chen, K. T. Chang, V. Y. Park, M. J. Kim, S. Chan, P. Chang, D. Chow, A. Luk, T. Kwong, and M. Y. Su. 2019. "Automatic Breast and Fibroglandular Tissue Segmentation in Breast MRI Using Deep Learning by a Fully-Convolutional Residual Neural Network U-Net." *Acad Radiol* 26 (11):1526-1535. doi: 10.1016/j.acra.2019.01.012.

## **AUTHOR BIOGRAPHIES**

**MOTAZ ALQAOUD** is a Ph.D. student in Biomedical Engineering in the Electrical and Computer Engineering Department at Old Dominion University. He holds an MS in Biomedical Engineering from New Haven University. His research interests lie in medical image modalities, surgery Planning, surgical navigation, and machine learning. His email address is [malqa004@odu.edu](mailto:malqa004@odu.edu).

**JOHN PLEMMONS, MD**, is an Assistant Professor in the Department of Radiology at Eastern Virginia Medical School. He completed his MD. Residency at the Department. Of Radiology from Eastern Virginia Medical School. He dedicates his professional life to helping early breast cancer diagnosis so that treatment has the greatest chance of success. His email address is [jkplemmons@gmail.com](mailto:jkplemmons@gmail.com).

**ERIC FELIBERTI, MD, FACS**, is a Professor and the Vice Chief of the Division of Surgical Oncology at Eastern Virginia Medical School. He completed his general surgical residency at the University of Texas Medical Branch. His research interests include cancer care, neuroendocrine tumors, peritoneal surface malignancies, and breast cancer. His email address is [felibeece@evms.edu](mailto:felibeece@evms.edu).

**KRISHNANAND KAIPA** received his Ph.D. in Aerospace Engineering from the Indian Institute of Science and is currently an Assistant Professor in the Mechanical & Aerospace Engineering Department at Old Dominion University. His research interests include collaborative robotics, cognitive robotics, swarm intelligence, and embodied cognition. His email address is [kkaipa@odu.edu](mailto:kkaipa@odu.edu).

**GABOR FICHTINGER** received his Ph.D. in Computer Science from the Technical University of Budapest, and currently is Professor and Canada Research Chair in Computer-Integrated Surgery, School of Computing at the Queen's University and holds a Cancer Ontario Research Chair in Cancer Imaging. His research interests include computer-Assisted surgery and interventions, scientific visualization, surgical planning and navigation, and medical robotics. His email address is [fichting@queensu.ca](mailto:fichting@queensu.ca).

**YIMMING XIAO** is an Assistant Professor in the Computer Science and Software Engineering department at Concordia University. He holds a Ph.D. in Biomedical Engineering from McGill University. His research interests include image-guided surgery, computer-assisted diagnosis, and machine learning. His email address is [yiming.xiao@concordia.ca](mailto:yiming.xiao@concordia.ca).

**SIQIN DONG** is a Ph.D. student in the Department of Mechanical & Aerospace Engineering at Old Dominion University. He holds a BE in Mechanical Design and Manufacturing Engineering from Central South Forestry University. His research interests include collaborative robotics, medical robotic and machine learning. His email address is [sdong002@odu.edu](mailto:sdong002@odu.edu).

**MICHEL AUDETTE** is an Associate Professor of Computational Modeling and Simulation Engineering and the Graduate Program Director of Biomedical Engineering at Old Dominion University. He holds a Ph.D. in Biomedical Engineering from McGill University. His research interests include medical/surgical simulation, surgery planning and navigation, and surgical robotics. His email address is [maudette@odu.edu](mailto:maudette@odu.edu).